

Full Paper

Inhibition mechanism of podocyte apoptosis in rats with membranous nephropathy by Chinese medicine Ke-mo-fang through integrin-linked kinase signalling pathway

Mingyu He¹, Shuai Zhang¹, Lindi Zhang², He Nan³, Di Jin³ and Shoulin Zhang^{3,*}

¹ College of Traditional Chinese Medicine, Changchun University of Chinese Medicine, Changchun 130117, China

² Pneumology Department, The Affiliated Hospital to Changchun University of Chinese Medicine, Changchun 130021, China

³ Nephrology Department, The Affiliated Hospital to Changchun University of Chinese Medicine, Changchun 130021, China

*Corresponding author, e-mail: zsl3692023@163.com

Received: 1 October 2024 / Accepted: 18 November 2024 / Published: 19 November 2024

Abstract: Membranous nephropathy (MN), a common pathological type of adult nephrotic syndrome, causes up to 30% of patients to progress to end-stage renal disease within 5-10 years. Podocyte injury and proteinuria are closely related to the occurrence and development of MN, and podocyte epithelial-mesenchymal transition (EMT) is the key factor leading to podocyte injury and proteinuria. Integrin-linked kinase (ILK) is a serine/threonine protein kinase with diverse biological activities. As an important downstream effector molecule of transforming growth factors - β 1 signalling pathway, ILK induces the specific expression of fibroblasts, accelerates the formation of renal interstitial fibrosis, and plays a role in the EMT of renal epithelial cells. Ke-mo-fang (KMF) is a traditional Chinese medicine formula, which has been used to delay the progression of worsening renal function. However, the therapeutic mechanism of KMF in MN remains unclear. In this study cationic bovine serum albumin was injected at multiple points subcutaneously in axilla, groin and tail vein to establish the MN rat mode. Thereafter, the KMF and ILK inhibitors (OSU-T315) were administered. Through the detection of serum indexes content, the expression of proteins related to kidney pathology, the podocyte function and the ILK signalling pathology, it was confirmed that KMF has a protective effect on podocytes of rats with MN by regulating the ILK signalling pathway, effectively preventing the progression of MN.

Keywords: Ke-mo-fang, podocyte apoptosis, membranous nephropathy, integrin-linked kinase

INTRODUCTION

Membranous nephropathy (MN) is a prevalent pathological type of adult nephrotic syndrome characterised by edema, significant proteinuria and persistent or intermittent microscopic hematuria. Recently, there has been a rapid increase in the incidence of MN in China, with an annual growth rate of 13%. It has become one of the primary glomerular diseases with a high occurrence rate, second only to IgA nephropathy [1, 2]. Approximately 30% of patients with MN will progress to end-stage renal disease within 5-10 years, leading to progressive renal failure and potential complications including death due to massive protein loss. Thromboembolic events are directly correlated with mortality [3-5] and significantly impact the quality of life, mortality rate, economic burden and overall human health.

The pathogenesis of MN is a complex process involving various factors such as different target antigens, genetic polymorphisms, genetic susceptibility and environmental factors [6-13]. Podocytes, located outside the glomerular basement membrane, play a crucial role in maintaining the permeability of the glomerular filtration membrane, synthesising components of the glomerular basement membrane, and supporting the capillary structure. It is widely believed that podocyte damage is closely associated with the development of MN. When immune complexes circulate or are deposited outside the glomerular basement membrane, the complement system is activated, leading to the formation of membrane attack complexes that can affect the morphology and function of podocytes [14]. The specific mechanisms underlying this process may involve oxidative stress, autophagy dysregulation, inflammation, abnormal expression of podocyte marker proteins, and epithelial-mesenchymal cell transdifferentiation [15].

Studies have confirmed that the occurrence and development of MN are associated with podocyte epithelial-mesenchymal transition (EMT) [16]. Changes in podocyte polarity, structural destruction and reduced function occur during EMT. This is accompanied by the abnormal expression of functional proteins such as nephrin, ZO-1, desmin, MMP-9 and α -SMA. Multiple factors contribute to this process, which ultimately leads to proteinuria and renal tissue damage. The transforming growth factors - β 1 (TGF- β 1)/smad signalling pathway, integrin-linked kinase (ILK) signalling pathway and Wnt/ β -catenin signalling pathway collectively regulate podocyte EMT. The ILK signalling pathway plays a crucial role in connecting and inducing various signalling pathways [17]. ILK, which is strongly expressed in glomerular podocytes, is activated through various pathways and is involved in various physiological and pathological renal processes. It has been found to be closely associated with MN and can contribute to the development of various kidney diseases including renal tumours, nephrotic syndrome, polycystic kidney disease and renal failure. Proteinuria, an independent risk factor for disease progression [18, 19], is closely linked to disease prognosis, and there is a positive correlation between ILK and changes in the 24-h urine protein (24h-UTP) level. Therefore, regulating the expression of the ILK signalling pathway is of great importance to reducing proteinuria, protecting podocytes and preventing renal fibrosis.

Traditional Chinese medicine has demonstrated multi-link and multi-target synergistic effects on the prevention and treatment of kidney diseases, particularly MN. Traditional Chinese medicine offers a safer and more effective approach to treating MN, compared to the use of hormones and immunosuppressants in Western medicine [20]. KMF consists of *Codonopsis pilosula* (Franch.), *Astragalus membranaceus*, *Coptis chinensis*, *Perilla frutescens*, *Rehmannia glutinosa*, *Ligusticum chuanxiong*, *Euryale ferox*, *Sabia japonica*, *Rhus chinensis*, *Lobelia chinensis* and *Oldenlandia diffusa*. It has found efficacy in effectively reducing edema and decreasing the

24h-UTP count in patients with MN in clinical practice. Hence this study aims to observe the impact of KMF on the expression of the main proteins of the ILK signalling pathway in an MN rat model through animal experiments, with the goal of exploring the molecular mechanism of this prescription in the treatment of MN.

MATERIALS

Laboratory Animals

Sixty-four adult male Sprague-Dawley rats weighing between 160–200 g and maintained under special pathogen-free conditions were provided by the Hubei Provincial Experimental Animal Research Center (Certificate No. SCXK 2020-0018). All rats were allowed free access to water and a standard laboratory diet in a special pathogen-free environment for 1 week. Qualitative urine protein and red blood cell counting experiments were conducted at the beginning and end of the first week, along with two 24h-UTP total protein tests. Rats with urine protein levels below 5 mg were included in the experiment. The animal experimental protocol of this study was reviewed and approved by the Experimental Animal Management and Use Committee of the Hubei Provincial Center for Disease Control and Prevention (Ethics Certificate No. 202220144).

Experimental Drugs

The KFM used was provided by the hospital affiliated to Changchun University of Traditional Chinese Medicine. It was composed of *Codonopsis pilosula* (20g), *Astragalus membranaceus* (30g), *Coptis chinensis* (3g), *Perilla frutescens* (6g), *Rehmannia glutinosa* (15g), *Ligusticum chuanxiong* (15g), *Euryale ferox* (15g), *Sabia japonica* (10g), *Rhus chinensis* (3g), *Lobelia chinensis* (15g) and *Oldenlandia diffusa* (15g). The dosage conversion was based on the findings of the 'Medical Experimental Zoology' study, which suggested that the dose for a 200-g rat is approximately 6.3 times that for a 70-kg human. For the experiment, 8.85 g/kg, 17.7 g/kg and 35.4 g/kg of the medicine were each dissolved in 2 mL of distilled water to create a suspension. This suspension was then administered orally once daily for 4 consecutive weeks. Benazepril hydrochloride (Shanghai Xinya Pharmaceutical Minhang Co., China) was also used in the study.

Experimental Reagents

The following were used in this study: cationised bovine serum albumin (C-BSA) prepared by Wuhan Lingsi Biotechnology Co., China; Freund's incomplete adjuvant obtained from Beyotime Biotechnology Co., China; 24h-UTP test kit purchased from Nanjing Jiancheng Bioengineering Institute, China; assay kits for serum creatinine (Scr), blood urea nitrogen (BUN), total cholesterol (TC), triglyceride (TG), alanine aminotransferase (ALT), aspartate aminotransferase (AST) and serum albumin (ALB) assessments acquired from Changchun Huili biotech Co., China; a phosphatase inhibitor and radio immunoprecipitation assay lysis buffer (phenylmethylsulfonyl fluoride, 100 mM, 1.5mL) obtained from Meilunbio Co., China; a cytoplasmic and nuclear protein extraction kit obtained from Jiangsu KeyGEN BioTECH Corp. Co., China; BCA protein concentration determination reagents A,B from GBCBIO Technologies Co., China).

The following rabbit polyclonal antibodies were used in this study: TGF- β 1, ZO-1 and desmin (Proteintech Group Co., China); nephrin (Beijing Bioss Co., China); MMP-9, anti- α -SMA, Snail and ILK (ABclonal Technology Co., China); glyceraldehyde-3-phosphate dehydrogenase (GAPDH) (Goodhere Biotech Co., China).

Additionally, the following reagents were used: blocked goat serum, neutral resin and hematoxylin-eosin staining solution (Wuhan Lingsi Biotechnology Co., China); hexamine silver iodate staining kit and Masson kit (BASO Co., China).

Main Instruments and Equipment

The following equipment was used in the study: H1-16KR desktop high-speed refrigerated centrifuge (Hunan Kecheng Instrument Equipment Co., China); JT-12J dehydrator and JB-P5 embedding machine (Wuhan Junjie Electronics Co. China); RM2016 pathology microtome (Shanghai Leica Instruments Co., China); TSY-B type decolourising shaker, MX-F type vortex mixer, and D1008E type handheld centrifuge (Wuhan Lingsi Biotechnology Co., China); Eclipse Ci type microscope, Eclipse CI type upright optical microscope, DS-Fi3 imaging system and DS-U3 imaging system (Nikon, Japan); SPX70BIII biochemical incubator, DK-20000-III electric thermostatic water bath (Fisford Instruments Co., China); TissueLyser-24L multi-sample tissue grinder (Shanghai Jingxin Industrial Development Co., China); 1410101 Multiskan FC microplate reader (Thermo Scientific Co., USA); Chemray240 fully automatic biochemical analyser (Rayto Life and Analytical Sciences Co., China); SH-523 type chemiluminescence imaging system (Hangzhou Shenhua Technology Co., China).

METHODS

Reagent Preparation

The C-BSA emulsifier configuration was as follows: 100 mg of C-BSA dry powder was mixed with 50 mL of physiological saline to prepare a C-BSA solution. This solution was then fully emulsified by adding an equal amount (50 mL) of Freund's incomplete adjuvant.

The C-BSA solution preparation process was as follows: 640 mg of C-BSA dry powder was thoroughly mixed with 100 mL of phosphate buffered saline (PBS). The resulting concentration was 6.4 mg/mL.

Regarding KMF, 450 mL of the original solution was collected. For the KMF high-dose (KMF-H) group, 200 mL of the original solution was diluted to a concentration of 7.43 g/mL. For the KMF medium-dose (KMF-M) group, 150 mL of the solution was diluted to a concentration of 3.72 g/mL. For the KMF low-dose (KMF-L) group, 100 mL of the solution was diluted to a concentration of 1.85 g/mL.

Regarding benazepril hydrochloride, 12.34 mg of benazepril hydrochloride tablets were dissolved in 98 mL of pure water by shaking. The resulting concentration was 0.126 mg/mL and the intragastric dose was 0.6 mg/kg.

Regarding the ILK inhibitor configuration, 144 mg of OSU-T315 was dissolved in 1 mL of DMSO by shaking. Subsequently, 195 mL of pure water was added to dilute the solution. The resulting concentration was 0.735 mg/mL and the intragastric dose was 3.5 mg/kg.

Animal Experiments

After 1 week of adaptive feeding, 64 healthy specific pathogen free male rats were included in the experiment. Eight rats were randomly selected for the normal control group and the remaining rats were subjected to modelling. For the modelling method, the modified Border method [21] was used to prepare C-BSA. This involved injecting the C-BSA emulsifier subcutaneously at multiple points in the rat's bilateral groin and axilla for pre-immunisation, with injections

administered once every alternate day for a week. Formal immunisation was conducted following pre-immunisation. The rats were injected with the C-BSA solution at a dose of 16 mg/kg through the tail vein three times a week for 4 weeks.

Successful modelling was considered if the rats in the model group tested positive for urine protein three times. The rats that were successfully modelled were then randomly divided into seven groups: the model group (Model); benazepril hydrochloride group (Benazepril); KMF-H, KMF-M, and KMF-L groups; OSU-T315+KMF-M group; and ILK inhibitor (OSU-T315) group. Each group comprised eight animals. The blank and model groups were administered distilled water by gavage at a volume of 2 mL per animal once daily for 4 weeks. The benazepril group received benazepril hydrochloride aqueous solution at a concentration of 0.6 mg/kg by gavage, with a gavage volume of 2 mL per animal once daily for 4 weeks. The KMF-H, KMF-M and KMF-L groups were administered KMF once a day for 4 weeks. The KMF-H group received a dose of 6.372 g/animal and a gavage volume of 4 mL/animal. The KMF-M group received a dose of 3.186 g/animal and a gavage volume of 2 mL/animal. The KMF-L group received a dose of 1.593 g/animal and an intragastric volume of 2 mL/animal. In the OSU-T315+KMF-M group, OSU-T315 was dissolved in 2 mL of distilled water at a concentration of 3.5 mg/kg to prepare a suspension. This suspension was then administered into the stomach along with 17.7 g/kg (3.186 g/animal) of KMF once daily for 4 weeks. In the OSU-T315 group, an OSU aqueous solution with a concentration of 0.735 mg/mL and a volume of 2 mL/animal was administered into the stomach once a day for 4 consecutive weeks.

Serum Biochemical Index Content Detection

Following the intervention, the rats in each group underwent a 12-hr fasting period. Subsequently, they were weighed and anaesthetised by the intraperitoneal administration of 30 mg/kg of sodium pentobarbital. The abdominal cavity of the rats was incised and blood was collected from the abdominal aorta and centrifuged. After standing for 30 min. the upper serum was separated by centrifugation at 3000 r/min. for 10 min. The blood biochemical indicators, i.e. BUN, ALT, AST, Scr, TC, TG and ALB levels, of each group were measured using a fully automatic biochemical analyser.

Observation of Pathological Morphology of Renal Tissues

Kidney specimens and blood samples were collected from anaesthetised rats. The kidneys were weighed and photographed against a monochromatic background. Half of the left kidney was fixed in 4% paraformaldehyde and subjected to a series of steps, i.e. dehydration, alcohol gradients, transparency, wax immersion and embedding. From the resulting 4- μ m sections, periodic acid-silver methenamine, hematoxylin-eosin, and Masson's trichrome staining were performed to observe the histological morphological changes in the rat kidneys, which were then documented through photographs. Other paraffin sections were subjected to routine dewaxing, hydration and high-pressure antigen retrieval. After cooling, the sections were washed with PBS and treated with 3% hydrogen peroxide solution. Subsequently, the sections were incubated with 10% goat serum, followed by the addition of primary antibodies (IgG, 1:100; C3, 1:100). After overnight incubation at 4°C, the sections were rinsed with PBS and incubated with the secondary antibody. The sections were then stained with 4',6-diamidino-2-phenylindole to label the nuclei, and excess reagent was washed away. Finally, the slides were washed with PBS on a destaining shaker. After the sections

were partially dried, an autofluorescence quenching agent was added to the samples and left to stand for 5 min. The sections were then rinsed with running water for 10 min. Subsequently, the sections were mounted with an anti-fluorescence quenching mounting medium, and the presence of IgG and complement 3 (C3) deposition was observed under an immunofluorescence microscope. Additionally, a portion of the kidney tissue was excised, cut into pieces and fixed in 2.5% glutaraldehyde. These samples were then examined under an electron microscope to observe changes in podocytes and the deposition of electron-dense matter.

Western Blot Analysis

The tissue blocks were washed 2–3 times with pre-cooled PBS, cut into small pieces and placed in a homogenisation tube. Homogenisation beads were then added. At the same time, 10 times the volume of radio immunoprecipitation assay lysis buffer was added for homogenisation. The tube was shaken repeatedly to ensure complete lysis and extraction of total protein from the kidney tissues. Furthermore, cytoplasmic and nuclear proteins were extracted from the rat kidney tissue cells and protein quantification was performed using the bicinchoninic acid method. For 5% SDS-PAGE gel electrophoresis, each sample contained 40 µg of total protein. The stacking gel voltage was set at 75 V while the separation gel voltage was set at 120 V. Electrophoresis was conducted until the bromophenol blue marker reached approximately 1 cm from the bottom. Following electrophoresis, membrane transfer was performed using the wet-transfer method. The membranes were blocked at room temperature for 30 min. The primary antibody was diluted according to the manufacturer's instructions and incubated overnight at 4°C on a shaker with slow shaking. After incubation, the membrane was washed with tris-buffered saline with Tween 20 and the secondary antibody (diluted at 1:10000) was added. The membrane was incubated at room temperature for 60 min. and washed thrice with tris-buffered saline with Tween 20. Finally, chemiluminescence colour development and enhanced chemiluminescence detection were performed, followed by the analysis of protein band gray values using Image-Pro Plus.

Immunofluorescence Analysis

Fresh kidney tissues were obtained and total RNA was extracted using the TRIzol method. Subsequently, cDNA was synthesised using reverse transcription for polymerase chain reaction. The internal reference GAPDH was utilised, and the 2- $\Delta\Delta$ CT method based on the Ct value of each sample ($\Delta\Delta$ Ct = Ct value of target gene - Ct value of internal reference gene) was employed for result processing and analysis. The primers were synthesised by General Biotech (Anhui) Co., China, as shown in Table 1.

Statistical Analysis

Data analysis was conducted using SPSS 26.0 statistical software. The values are expressed as mean \pm standard deviation ($\bar{x}\pm s$). Prior to the analysis, the measurement data were assessed for normality and homogeneity of variances. When variances were found to be homogeneous, comparisons between multiple groups were performed using single-factor analysis of variance and inter-group analysis. For multiple comparisons, the least significant difference t-test was used, whereas the rank-sum test was used in the case of uneven variances. The level of statistical significance was set at $P < 0.05$.

Table 1. Primer sequence

Name	Primer	Sequence	Size/Bp
GAPDH	Forward	ACAGCAACAGGGTGGTGGAC	253
	Reverse	TTTGAGGGTGCAGCGAACTT	
TGF- β 1	Forward	CACTCCCGTGGCTTCTAGTG	145
	Reverse	GGACTGGCGAGCCTTAGTTT	
Nephrin	Forward	CGGAGAACAAGAACGTGACC	177
	Reverse	ATTGTCTTCTCTCCGCACCA	
ZO-1	Forward	TCATCTCCAGTCCCTTACCTTTC	276
	Reverse	ATGGTTTTGTCTCATCATTTCCTCA	
Desmin	Forward	GGACATCCGTGCTCAGTAT	276
	Reverse	CAATCTCGCAGGTGTAGG	
MMP-9	Forward	CAACTCGGCAGGAGAGATGT	177
	Reverse	TCCGGCACTGAAGAATGATC	
α -SMA	Forward	GCATCCACGAAACCACCTAT	253
	Reverse	GAGCCGCCGATCCAGACAGA	
Snail	Forward	GTTACCTTCCAGCAGCCCTAC	145
	Reverse	TTTGCCACTGTCCTCATCG	

RESULTS

Effects of KMF on 24h-UTP Level in Rats with MN

Before modelling, there was no statistically significant difference in the 24h-UTP levels among the rats in each group. After 4 weeks of modelling, the group of drug-treated rats showed a significant increase in 24h-UTP levels compared to the blank group ($P < 0.05$). However, after 2 weeks of administration, the 24h-UTP levels of rats in the traditional Chinese medicine and benazepril groups decreased significantly compared with those in the model group ($P < 0.05$). Furthermore, the KMF groups exhibited significant differences compared to the benazepril group ($P < 0.05$). After 4 weeks of administration, significant differences were observed between the KMF and benazepril groups compared to the model group ($P < 0.05$). However, no significant differences were observed between the KMF-H and benazepril groups (Figure 1).

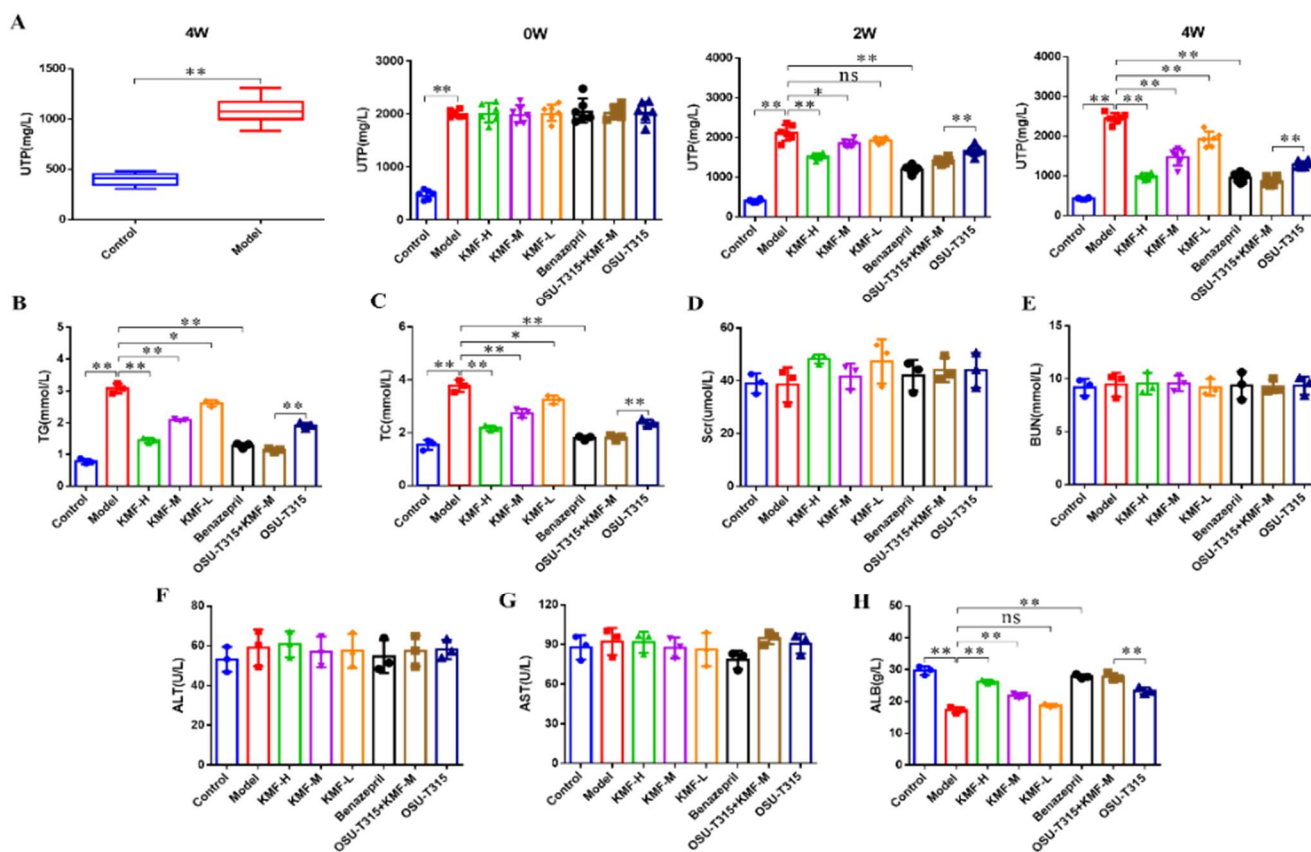


Figure 1. Effects of KMF on serum ALT, AST, ALB, TC, TG, BUN and Scr contents at 24h-UTP levels in MN model rats: (A) Changes in 24h-UTP levels in MN rats at 0W, 2W, 4W after confirmation of successful modelling and 4w after formal immunisation; (B, C, D, E, F, G and H respectively): Changes in serum TG, TC, Scr, BUN, ALT, AST and ALB levels of rats in each group (n=8). Note: *statistical difference ($P < 0.05$), **statistical difference ($P < 0.01$), ns = no statistical difference ($P > 0.05$)

Effects of KMF on Serum ALT, AST, ALB, TC, TG, BUN and Scr levels in Rats with MN

The serum ALT, AST, ALB, TC, TG, BUN and Scr levels of the rats in each group were within the normal range. Compared with the blank group, there were no significant differences in the serum ALT, AST, BUN and Scr levels of rats in the model group ($P > 0.05$). However, the levels of ALB, TC and TG significantly increased ($P < 0.05$). Compared with the model group, there were no significant differences in the serum ALT, AST and BUN levels among rats in the KMF, benazepril, OSU-T315+KMF-M and OSU-T315 groups ($P > 0.05$). However, the serum Scr levels in rats in the KMF-H group showed a significant increase ($P < 0.05$). Additionally, the TC and TG levels in the serum of rats in the KMF, OSU-T315+KMF-M and OSU-T315 groups significantly decreased ($P < 0.05$). Furthermore, the ALB levels in the serum of rats in the KMF, benazepril, OSU-T315+KMF-M and OSU-T315 groups significantly increased ($P < 0.05$) (Figure 1).

KMF Ameliorated Glomerular Pathomorphology in Rats with MN

Hematoxylin-eosin staining revealed no significant pathological, structural or morphological changes in rats in the blank group. However, in the model group the rats exhibited an increase in glomerular volume, irregular arrangement of foot processes, fusion and disappearance of some foot

processes, and significant thickening of the basement membrane. In contrast, the KMF, benazepril, OSU-T315+KMF-M and OSU-T315 groups exhibited improvements in pathological damage, such as glomerular basement membrane thickening and foot process fusion (Figure 2).

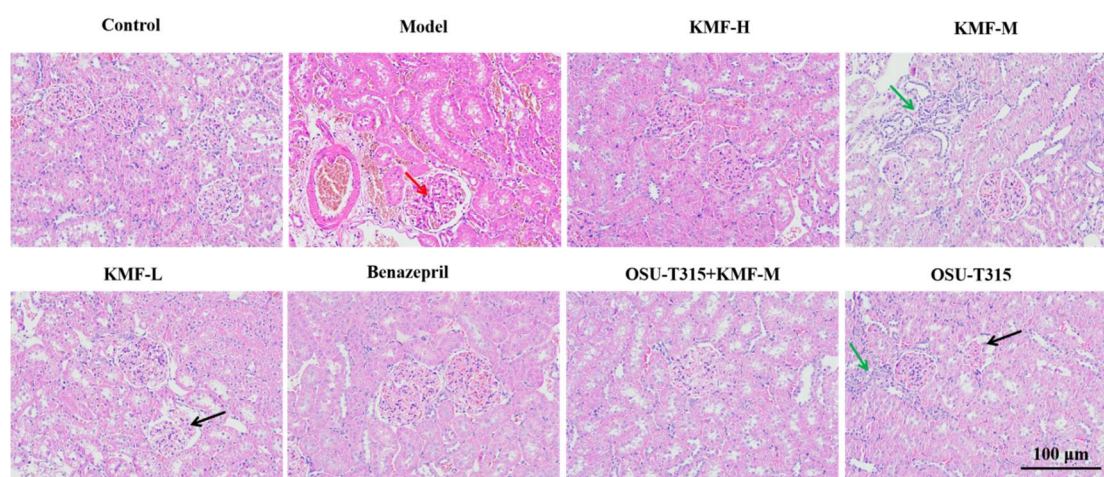


Figure 2. Hematoxylin-eosin staining on kidney tissue of each group and histopathological changes observed under optical microscope (screen magnification = $\times 100$, scale bar = 100 μm).

Periodic acid-silver methenamine staining revealed that the glomeruli in the control group displayed no thickening of the basement membrane, normal epithelial cell structure, and no fibrosis. In contrast, the model group exhibited significant thickening of the glomerular basement membrane and vacuolar degeneration of the renal tubular epithelial cells. However, the KMF, benazepril, OSU-T315+KMF-M and OSU-T315 groups exhibited a reduction in glomerular basement membrane thickening and a reduction in the degree of vacuolar degeneration of renal tubular epithelial cells (Figure 3).

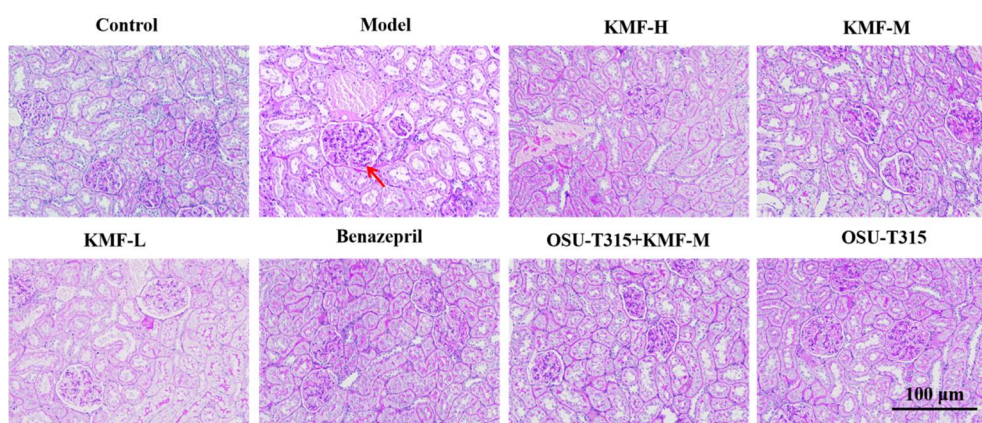


Figure 3. Periodic acid-silver methenamine staining on kidney tissue of each group and histopathological changes observed under optical microscope (screen magnification = $\times 100$, scale bar = 100 μm).

Masson's trichome staining revealed that the size, shape and structure of the glomeruli in the blank group were normal. Compared to the blank group, the model group exhibited a significantly thickened glomerular basement membrane with evident vacuolar degeneration and deposition of granular fuchinophilic substances beneath the epithelium. The degree of glomerular damage was

significantly reduced in the KMF, benazepril, OSU-T315+KMF-M and OSU-T315 groups compared with that in the model group (Figure 4).

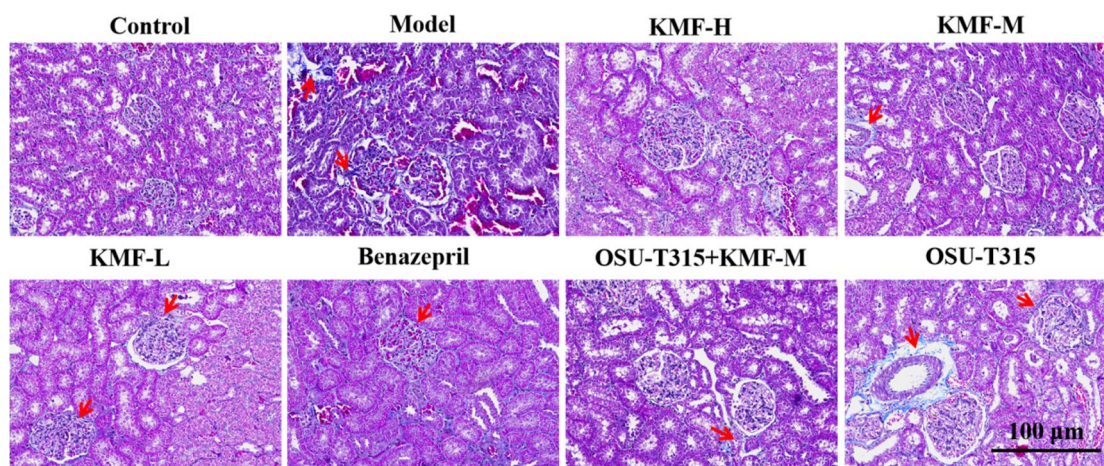


Figure 4. Masson's staining performed on kidney tissue of each group and histopathological changes observed under optical microscope (screen magnification = $\times 100$, scale bar = $100\mu\text{m}$)

Effects of KMF on Transcription of ILK Signal Pathway-related Proteins

The quantitative real-time PCR (qRT-PCR) method gave the following results. Compared with the blank group, the mRNA transcription of nephrin and ZO-1 was significantly reduced in the model group ($P < 0.05$). Additionally, the mRNA transcription of TGF- $\beta 1$, desmin, MMP-9, α -SMA and Snail was significantly increased ($P < 0.05$). Compared to the model group, the KMF group showed a decrease in the mRNA transcription of TGF- $\beta 1$, desmin, MMP-9, α -SMA and Snail while the mRNA transcription of nephrin and ZO-1 increased. Notably, the KMF-H group exhibited the most significant change ($P < 0.05$). The benazepril and OSU-T315+KMF-M groups also exhibited a significant decrease in the mRNA transcription of TGF- $\beta 1$, desmin, MMP-9, α -SMA and Snail ($P < 0.05$) while the mRNA transcription of nephrin and ZO-1 significantly increased ($P < 0.05$). The OSU-T315 group displayed a decrease in the mRNA transcription of TGF- $\beta 1$, desmin, MMP-9, α -SMA and Snail, with desmin showing a more significant decrease ($P < 0.05$). In contrast, the mRNA transcription of nephrin and ZO-1 increased, with nephrin showing a more significant increase ($P < 0.05$) (Figure 5).

Western Blot Analysis of Expression of TGF- $\beta 1$, Nephrin, ZO-1, Desmin, MMP-9, α -SMA, Snail and ILK

Compared to the control group, the model group showed a significant increase in the protein expression of TGF- $\beta 1$, MMP-9, desmin, α -SMA, Snail and ILK in the kidney tissues of the rats ($P < 0.05$). Conversely, the expression of nephrin and ZO-1 significantly decreased ($P < 0.05$).

Compared to the model group, the KMF and OSU-T315+KMF-M groups exhibited a significant decrease in the expression of TGF- $\beta 1$, MMP-9, desmin, α -SMA, Snail and ILK proteins in the kidney tissues of the rats, while the expression of nephrin and ZO-1 significantly increased ($P < 0.05$). Furthermore, the benazepril group exhibited a significant increase in the expression of TGF- $\beta 1$, MMP-9, desmin, α -SMA and Snail in the kidney tissues ($P < 0.05$), along with a significant increase in the expression of nephrin and ZO-1 ($P < 0.05$) (Figures 6 and 7).

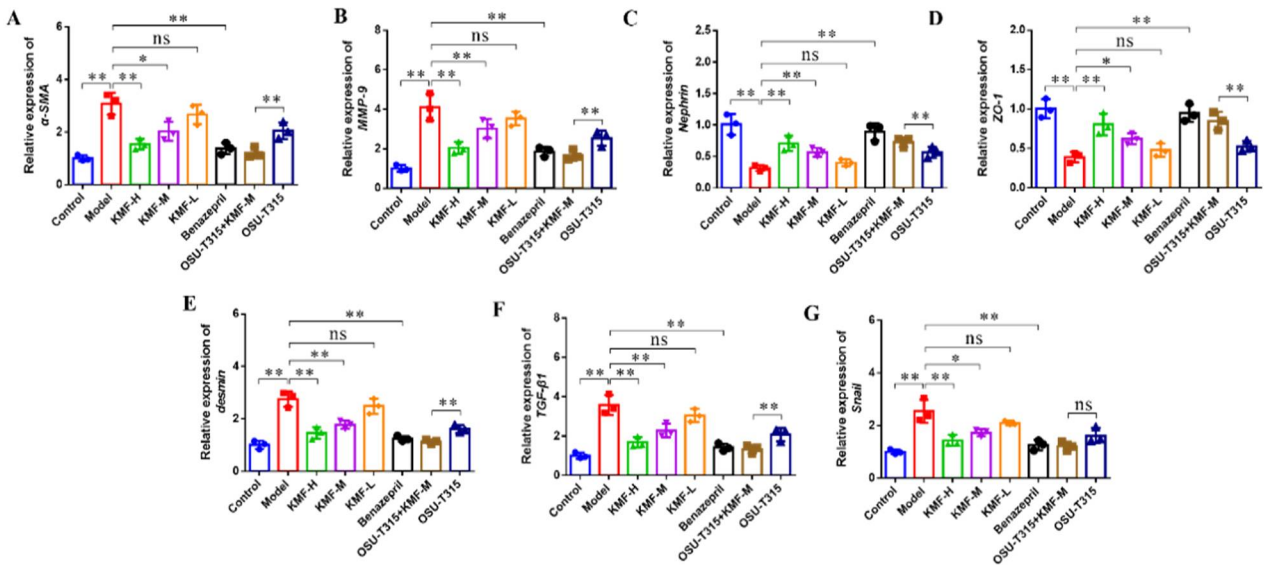


Figure 5. Results of qRT-PCR method employed to examine the transcription of proteins associated with ILK signalling pathway using KMF. The histogram illustrates the expression levels of α -SMA, MMP-9, nephrin, ZO-1, desmin, TGF- β 1 and Snail mRNS (A-G respectively) in each group. Note: * statistical difference ($P < 0.05$), ** highly significant statistical difference ($P < 0.01$), ns = no statistical difference ($P > 0.05$)

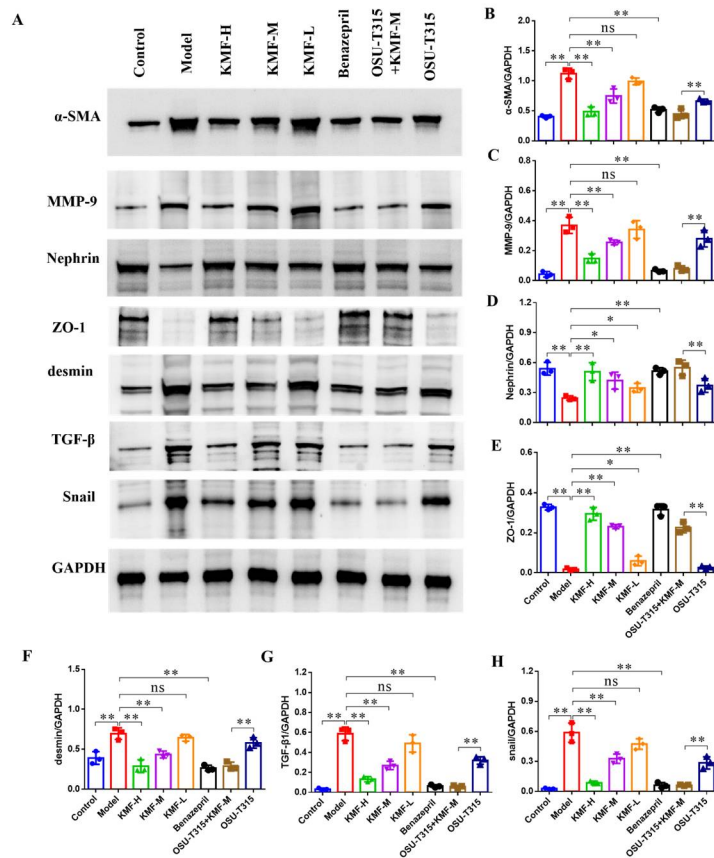


Figure 6. Results of Western Blot method analysis of expression of TGF- β 1, nephrin, ZO-1, desmin, MMP-9, α -SMA and Snail (B-H respectively) in renal tissue of rats in each group. Note: *statistical difference ($P < 0.05$), **statistical difference ($P < 0.01$), ns = no statistical difference ($P > 0.05$)

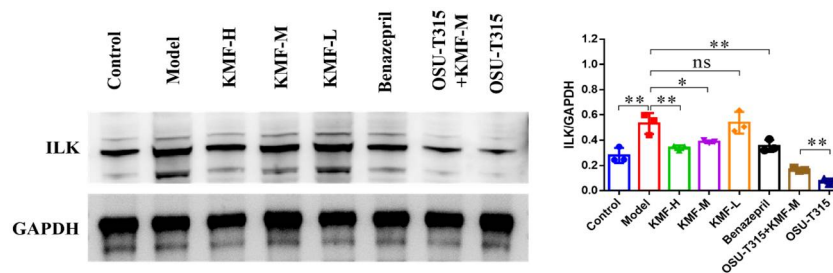


Figure 7. Results of Western Blot method analysis of expression of ILK in kidney tissue of rats in each group. Note: * statistical difference ($P < 0.05$), ** statistical difference ($P < 0.01$), ns = no statistical difference ($P > 0.05$)

DISCUSSION AND CONCLUSIONS

This study aims to observe the protective mechanism of KMF in the podocytes of rats with MN. EMT is one of the important forms of podocyte injury, which is also one of the key factors leading to the progressive development of proteinuria and MN. When podocytes are damaged, the basement membrane of glomerular capillaries will display diffused spike formation or uneven thickening, significantly increased mesenchymal proteins, granular deposition of IgG and C3 on the wall of glomerular capillaries, diffused fusion of foot process, abnormal expression of related proteins, and activation of the ILK signalling pathway, eventually leading to the structural destruction and dysfunction of podocytes, massive protein losses, and gradual renal fibrosis. Therefore, further research on the specific mechanism of podocyte injury and the methods for blocking or inhibiting podocyte injury is the key to delaying MN progression. Among them, the ILK signalling pathway has been verified in the experiments. These findings may provide a scientific basis for the clinical use of KMF as a potential treatment option for patients with MN.

In the EMT process the expression levels of podocyte-related proteins antagonise those of mesenchymal proteins. Previous studies have confirmed that nephrin and ZO-1 are highly expressed in podocytes of normal renal tissues, whereas desmin, MMP-9 and α -SMA are lowly expressed; in contrast, nephrin and ZO-1 are lowly expressed in podocytes of MN patients, whereas TGF- β 1, desmin, MMP-9, α -SMA, Snail and ILK are highly expressed [21, 22]. This will activate the ILK signalling pathway, the key signalling pathway of podocyte EMT, resulting in the abnormal expression of its downstream factors nephrin, ZO-1, desmin, MMP-9 and α -SMA. Most of these factors are expressed in the glomerular capillary loops of podocytes, which will directly affect the structural integrity of interprocess slit membrane of podocytes, promote the transformation of renal proper cells into myofibroblasts, stimulate the expression of Snail, the key factor for podocyte EMT, and further accelerate the process of renal fibrosis. At the same time, the high expression of TGF- β 1 is the most important pro-inflammatory product produced during complement activation, which also plays an important role in forming membrane attack complex C5b-9 and accelerating glomerular fibrosis and renal dysfunction. The ILK inhibitor OSU-T315 is one of the currently available drugs.

As indicated in some studies [23-25], OSU-T315 can specifically inhibit the expression of ILK signal, which can thereby affect the expression of key factors in the upstream and downstream of the ILK signalling pathway, reduce the occurrence of inflammatory response and glomerular podocyte fibrosis, mitigate the degree of MN proteinuria, and delay renal functional deterioration. However, due to too few experimental and clinical studies, it can hardly be widely used, its safety and effectiveness remain unclear, and whether it can maximise the benefits for patients cannot be

guaranteed. In this case the advantages of traditional Chinese medicine in the treatment of MN gradually emerge. This study has found that KMF can improve the expression levels of nephrin and ZO-1 proteins in the renal tissues of rats with MN, reduce those of desmin, MMP-9 and α -SMA proteins, and down-regulate the key factors of the ILK signalling pathway. Consequently, KMF can alleviate podocyte damage by reducing the expression levels of key factors in the ILK signalling pathway and have a protective effect on model rats with MN.

Nonetheless, there are some limitations in this study. First, it only investigated the mechanism of KMF in inhibiting podocytic apoptosis at the animal experimental level *in vivo*, which should be further verified and explored through *in vitro* cell experiments. Second, podocyte injury is also closely related to autophagy, immune inflammation and pyroptosis. Whether KMF affects MN by regulating autophagy, immune inflammation and pyroptosis needs to be further explored [26-27].

To sum up, this study has demonstrated that KMF can enhance proteinuria in rats with MN by regulating the expression of relevant proteins in the kidney, inhibiting podocyte EMT, safeguarding the structure and function of podocytes, and restraining the progression of renal fibrosis and edema. The underlying mechanism may be associated with the deactivation of the ILK signalling pathway. Considering the intricate pathogenesis of MN, future research should focus on tissue transcriptome sequencing and pathway enrichment to further investigate the mechanism of action of KMF in the treatment of MN and its influence on the IKL signalling pathway.

ACKNOWLEDGEMENTS

This work was supported by the Scientific and Technological Development Plan Projects of Jilin Province (Project No.YDZJ202301ZYTS145).

Author contributions

S. Z. and M. H. designed this study and assisted with animal experiments. L. Z., D. J. and H. N. interpreted the data and modified the manuscript. M. H. and S. Z. wrote the manuscript. All the authors reviewed the final version of the manuscript and agreed to publication. M. H. and S. Z. contributed equally to this work.

REFERENCES

1. X. Xu, G. Wang, N. Chen, T. Lu, S. Nie, G. Xu, P. Zhang, Y. Luo, Y. Wang, X. Wang, J. Schwartz, J. Geng and F. F. Hou, "Long-Term Exposure to Air Pollution and Increased Risk of Membranous Nephropathy in China", *J. Am. Soc. Nephrol.*, **2016**, 27, 3739-3746.
2. T. Chen, Y. Zhou, X. Chen, B. Chen and J. Pan, "Acute kidney injury in idiopathic membranous nephropathy with nephrotic syndrome", *Ren. Fail.*, **2021**, 43, 1004-1011.
3. B. E. Marx and M. Marx, "Prediction in idiopathic membranous nephropathy", *Kidney Int.*, **1999**, 56, 666-673.
4. S. L. Hogan, K. E. Muller, J. C. Jennette and R. J. Falk, "A review of therapeutic studies of idiopathic membranous glomerulopathy", *Am. J. Kidney Dis.*, **1995**, 25, 862-875.
5. R. J. Glasscock, "Diagnosis and natural course of membranous nephropathy", *Semin. Nephrol.*, **2003**, 23, 324-332.
6. L. H. Beck Jr., R. G. B. Bonegio, G. Lambeau, D. M. Beck, D. W. Powell, T. D. Cummins, J. B. Klein and D. J. Salant, "M-type phospholipase A2 receptor as target antigen in idiopathic membranous nephropathy", *N. Engl. J. Med.*, **2009**, 361, 11-21.

7. Y. Pan, J. Wan, Y. Liu, Q. Yang, W. Liang, P. C. Singhal, M. A. Saleem and G. Ding, “sPLA2 IB induces human podocyte apoptosis via the M-type phospholipase A2 receptor”, *Sci. Rep.*, **2014**, 4, Art.no.6660.
8. S. M. Maifata, R. Hod, F. Zakaria and F. A. Ghani, “Role of Serum and Urine Biomarkers (PLA2R and THSD7A) in Diagnosis, Monitoring and Prognostication of Primary Membranous Glomerulonephritis”, *Biomolecules*, **2020**, 10, Art.no.319.
9. P. D. Burbelo, M. Joshi, A. Chaturvedi, D. J. Little, J. S. Thurlow, M. Waldman and S. W. Olson, “Detection of PLA2R Autoantibodies before the Diagnosis of Membranous Nephropathy”, *J. Am. Soc. Nephrol.*, **2020**, 31, 208-217.
10. S. Kim, H. J. Chin, K. Y. Na, S. Kim, J. Oh, W. Chung, J. W. Noh, Y. K. Lee, J. T. Cho, E. K. Lee and D. W. Chae, “Single nucleotide polymorphisms in the phospholipase A2 receptor gene are associated with genetic susceptibility to idiopathic membranous nephropathy”, *Nephron. Clin. Pract.*, **2011**, 117, c253-c258.
11. Y. H. Liu, C. H. Chen, S. Y. Chen, Y. J. Lin, W. L. Liao, C. H. Tsai, L. Wan and F. J. Tsai, “Association of phospholipase A2 receptor 1 polymorphisms with idiopathic membranous nephropathy in Chinese patients in Taiwan”, *J. Biomed. Sci.*, **2010**, 17, Art.no.81.
12. W. G. Couser and R. J. Johnson, “The etiology of glomerulonephritis: Roles of infection and autoimmunity”, *Kidney Int.*, **2014**, 86, 905-914.
13. A. E. van de Logt, M. Fresquet, J. F. Wetzels and P. Brenchley, “The anti-PLA2R antibody in membranous nephropathy: What we know and what remains a decade after its discovery”, *Kidney Int.*, **2019**, 96, 1292-1302.
14. V. P. Romanov and S. A. Klopotskiĭ, “Paraneoplastic membranous nephropathy”, *Klin. Med (Mosk)*, **2006**, 84, 59-61.
15. X. Li, G. P. Lei, Z. Feng, T. Wang and S. Dong, “Traditional Chinese Medicine Intervention in membranous nephropathy based on podocyte injury: A review”, *Chinese J. Exp. Trad. Med. Form.*, **2023**, 24, 257-264.
16. M. Lei, “To investigate the mechanism of Fuzhengqufeng prescription in treating membranous nephropathy rats based on regulation of podocyte transdifferentiation”, Beijing University of Chinese Medicine, Chaoyang, China, **2020**.
17. J. Zhao and Z. J. Zhao, “Research progress on molecular mechanism of epithelial-mesenchymal transdifferentiation of podocytes and Chinese medicine intervention”, *Chinese J. Integr. Trad. Western Nephrol.*, **2014**, 15, 1119-1122 (in Chinese).
18. S. J. Shankland, “The podocyte's response to injury: Role in proteinuria and glomerulosclerosis”, *Kidney Int.*, **2006**, 69, 2131-2147.
19. R. C. Wiggins, “The spectrum of podocytopathies: A unifying view of glomerular diseases”, *Kidney Int.*, **2007**, 71, 1205-1214.
20. Y. P. Chen, Y. Y. Deng, Z. H. Ni and T. Wang, “A prospective, randomized, controlled, multicenter clinical study on the treatment of nephrotic syndrome with traditional Chinese medicine in idiopathic membranous nephropathy”, *Chinese J. Integr. Trad. Western Nephrol.*, **2012**, 13, 471-474 (in Chinese).
21. J. Liang, Y. Zhang, Y. R. Zhao, X. L. Meng and L. Wang, “Model rats with membranous nephropathy induced by cationic bovine serum albumin: Expressions of related proteins in podocytes”, *Chinese J. Tissue Eng. Res.*, **2016**, 53, 6028-6033 (in Chinese).
22. T. Wang, Z. Feng, J. Wu, G. P. Lei and S. Dong, “Effects of Qidi Gushen recipe on the expression of podocyte Hiatus membrane proteins nephrin and podocin in renal tissue of rats with membranous nephropathy”, *Prog. Modern Biomed.*, **2022**, 22, 4043-4048.
23. W. Lu, S. Gong, J. Li, H. Luo and Y. Wang, “Efficacy and safety of rituximab in the treatment of membranous nephropathy: A systematic review and meta-analysis”, *Medicine (Baltimore)*, **2020**, 99, Art.no.e19804.
24. J. Song, Y. Wang, C. Liu, Y. Huang, L. He, X. Cai, J. Lu, Y. Liu and D. Wang, “Cordyceps militaris

fruit body extract ameliorates membranous glomerulonephritis by attenuating oxidative stress and renal inflammation via the NF- κ B pathway”, *Food Funct.*, **2016**, 7, 2006-2015.

25. A. Howman, T. L. Chapman, M. M. Langdon, C. Ferguson, D. Adu, J. Feehally, G. J. Gaskin, D. R. Jayne, D. O'Donoghue and M. Boulton-Jones, “Immunosuppression for progressive membranous nephropathy: A UK randomised controlled trial”, *Lancet*, **2013**, 381, 744-751.
26. L. J. Yin, L. Yu, J. C. He and A. Chen, “Controversies in podocyte loss: Death or detachment”, *Front. Cell Dev. Biol.*, **2021**, 9, Art.no.771931.
27. C. Yang, Z. Zhang, J. Liu, P. Chen, J. Li, H. Shu, Y. Chu and L. Li, “Research progress on multiple cell death pathways of podocytes in diabetic kidney disease”, *Mol Med.*, **2023**, 29, Art.no.135.

© 2024 by Maejo University, San Sai, Chiang Mai, 50290 Thailand. Reproduction is permitted for noncommercial purposes.